4

POWER SYSTEM STABILIZERS

Power system stabilizer (PSS) controller design, methods of combining the PSS with the excitation controller (AVR), investigation of many different input signals and the vast field of tuning methodologies are all part of the PSS topic. This thesis is an investigation into modifying the input of a specific type of PSS as applied to a power system, and is not intended to serve as an exhaustive review of the domain of PSS application and design. The references related to this topic, [18-29], provide a survey of the state-of-the-art of this topic. This chapter will focus on providing a review of a few of the technologies and approaches, with the goal of making the case for using this type of controller to solve the low frequency inter-area oscillation problem. Details such as the type of PSS structure selected, tuning methods for controllers with and without the use of SPMs, and input signals considered are given in Chapter 6.

4.1 Control Action and Controller Design

The action of a PSS is to extend the angular stability limits of a power system by providing supplemental damping to the oscillation of synchronous machine rotors through the generator excitation. This damping is provided by a electric torque applied to the rotor that is in phase with the speed variation. Once the oscillations are damped, the thermal limit of the tie-lines in the system may then be approached. This supplementary control is very beneficial during line outages and large power transfers [23,24]. However, power system instabilities can arise in certain circumstances due to negative damping effects of the PSS on the rotor. The reason for this is that PSSs are tuned around a steady-state operating point; their damping effect is only valid for small excursions around this operating point. During severe disturbances, a PSS may actually cause the generator under its control to lose synchronism in an attempt to control its excitation field [24].

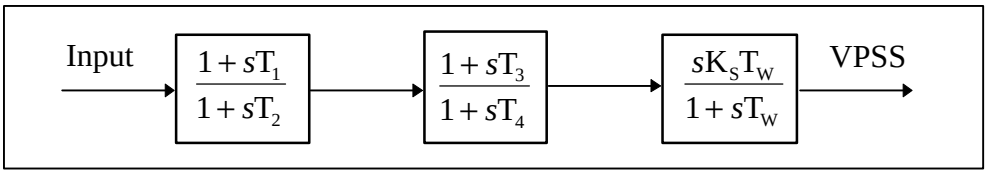

Figure 4.1: Lead-Lag Power System Stabilizer [23]

A "lead-lag" PSS structure is shown in Figure 4.1. The output signal of any PSS is a voltage signal, noted here as VPSS(s), and added as an input signal to the AVR/exciter. For the structure shown in Figure 4.1, this is given by

$$\mathrm{VPSS}(s) = \frac{sK_S T_W}{(1+sT_W)} \frac{(1+sT_1)}{(1+sT_2)} \frac{(1+sT_3)}{(1+sT_4)} \mathrm{Input}(s) \qquad (4.1)$$

This particular controller structure contains a washout block, $sT_W/(1+sT_W)$, used to reduce the over-response of the damping during severe events. Since the PSS must produce a component of electrical torque in phase with the speed deviation, phase lead blocks circuits are used to compensate for the lag (hence, "lead-lag') between the PSS output and the control action, the electrical torque. The number of lead-lag blocks needed depends on the particular system and the tuning of the PSS. The PSS gain K_S is an important factor as the damping provided by the PSS increases in proportion to an increase in the gain up to a certain critical gain value, after which the damping begins to decrease. All of the variables of the PSS must be determined for each type of generator separately because of the dependence on the machine parameters. The power system dynamics also influence the PSS values. The determination of these values is performed by many different types of tuning methodologies, as will be shown in Section 4.3.

Other controller designs do exist, such as the "desensitized 4-loop" integrated AVR/PSS controller used by *Electricité de France* [26] and a recently investigated proportional-integral-derivative (PID) PSS design [27]. Differences in these two designs lie in their respective tuning approaches for the AVR/PSS ensemble; however, the performance of both structures is similar to those using the lead-lag structure.

4.2 Input Signals

The input signal for the PSSs in the system is also a point of debate. The signals that have been identified as valuable include deviations in the rotor speed ($\Delta\omega = \omega_{mach} - \omega_o$), the frequency ($\Delta f$), the electrical power (ΔPe) and the accelerating power (ΔPa). Since the main action of the PSS is to control the rotor oscillations, the input signal of rotor speed has been the most frequently advocated in the literature [1,11]. Controllers based on speed deviation would ideally use a differential-type of regulation and a high gain. Since this is impractical in reality, the previously mentioned lead-lag structure is commonly used. However, one of the limitations of the speed-input PSS is that it may excite torsional oscillatory modes [11,23].

A power/speed (ΔPe-ω, or delta-P-omega) PSS design was proposed as a solution to the torsional interaction problem suffered by the speed-input PSS [25]. The power signal used is the generator electrical power, which has high torsional attenuation. Due to this, the gain of the PSS may be increased without the resultant loss of stability, which leads to greater oscillation damping [11].

A frequency-input controller has been investigated as well. However, it has been found that frequency is highly sensitive to the strength of the transmission system - that is, more sensitive when the system is weaker - which may offset the controller action on the electrical torque of the

machine [23]. Other limitations include the presence of sudden phase shifts following rapid transients and large signal noise induced by industrial loads [11]. On the other hand, the frequency signal is more sensitive to inter-area oscillations than the speed signal, and may contribute to better oscillation attenuation [23-25].

The use of a power signal as input, either the electrical power (ΔPe) or the accelerating power ($\Delta Pa = P_{mech} - P_{elec}$), has also been considered due to its low level of torsional interaction. The ΔPa signal is one of the two involved in the "4-loop" AVR/PSS controller from [26], even though the tuning method related to this design approach is valid for other input signals.

4.3 Control and Tuning

The conflicting requirements of local and inter-area mode damping and stability under both small-signal and transient conditions have led to many different approaches for the control and tuning of PSSs. Methods investigated for the control and tuning include state-space/frequency domain techniques [19,20], residue compensation [22], phase compensation/root locus of a lead-lag controller [23-25], desensitization of a robust controller [26], pole-placement for a PID-type controller [27], sparsity techniques for a lead-lag controller [28] and a strict linearization technique for a linear quadratic controller [29]. The diversity of the approaches can be accounted for by the difficulty of satisfying the conflicting design goals, and each method having its own advantages and disadvantages. This is the crux of the problem of low frequency oscillation damping by the application of power system stabilizers.

This thesis is not intended to provide a qualitative analysis of each of these techniques; rather, the improvement of the oscillation damping and resulting stability improvement of an existing PSS design through the use of synchronized phasor measurements is the final goal. Through the analysis performed here, it will be shown that the use of synchronized phasor measurements can improve the damping of an inter-area mode beyond that of an "optimally" tuned PSS. It will also be shown that the local and inter-area modes are effectively decoupled, without a loss of stability of either mode.

5

POWER SYSTEM MODELING

This chapter presents the models used for the generator, turbine and speed governor, automatic voltage regulators and power system stabilizers followed by a detailed description of the two-area, 4-machine test power system.

5.1 Generator Model

There are several models which have been used in modeling synchronous machines for stability studies, some including damper windings and transient flux linkages, some neglecting them. A two-axis model that includes one damper winding in the d-axis (direct axis) and two in the q-axis (quadrature axis) along with the transient and sub-transient characteristics of the machine is used in EUROSTAG [30,31,32], the software package used in part for this research. This model will be discussed here and involves the transformation of the machine variables to a common rotor-based reference frame through the Park's transformation [11,30,33]. This transformation changes a reference frame fixed with the stator to a rotating reference frame fixed with respect to the rotor, namely the direct axis (*d*-axis), the quadrature axis (*q*-axis) and a third axis associated with the zero sequence component current (*0*-axis). Eventually, the latter is dropped from the model due the fact that the zero sequence current is equal to zero for a balanced system.

The *dq*-axis model includes the transient and sub-transient characteristics of the machine. The latter are governed by

$$u_d = -r_a i_d + \omega\lambda_q - \dot{\lambda}_d \tag{5.1}$$

$$u_q = -r_a i_q + \omega\lambda_d - \dot{\lambda}_q \tag{5.2}$$

$$u_f = r_f i_f + \dot{\lambda}_f \tag{5.3}$$

$$0 = r_D i_D + \dot{\lambda}_D \tag{5.4}$$

$$0 = r_{Q1} i_{Q1} + \dot{\lambda}_{Q1} \tag{5.5}$$

$$0 = r_{Q2} i_{Q2} + \dot{\lambda}_{Q2} \tag{5.6}$$

The common flux terms are

$$\lambda_{AD} = M_d\left(i_d + i_f + i_D\right) \tag{5.7}$$

$$\lambda_{AQ} = M_q\left(i_q + i_{Q1} + i_{Q2}\right) \tag{5.8}$$

Once the non-state *d*- and *q*-axis variables have been eliminated, these equations will encompass four state variables per machine. The final two state equations are provided by the rotor swing equation in first order, ODE form:

$$2H\dot{\omega} = T_M - T_E = T_M - \lambda_q i_d - \lambda_d i_q \tag{5.9}$$

$$\dot{\Theta} = \omega_o \omega \tag{5.10}$$

These equations represent the $\dot{\mathbf{x}} = \mathbf{f}(\mathbf{x},\mathbf{u})$ model of the system. The final form of these state equations is given after the linearization is performed in Section 5.5. The variable definitions for (5.1) - (5.10) are summarized in Table 5.1.

Variable	Units	Definitions
x_d, x_q	pu	d- and q-axes synchronous reactances
x'_d, x'_q	pu	d- and q-axes transient reactances
x''_d, x''_q	pu	d- and q-axes sub-transient reactances
Ra	pu	stator resistance
Xl	pu	stator leakage inductance
T'_{do}, T'_{qo}	sec	d- and q-axes transient open circuit time constant
T''_{do}, T''_{qo}	sec	d- and q-axes sub-transient open circuit time constant
H	pu sec	stored energy at rated speed, inertia constant
u_d, u_q, u_f	pu	d-axis, q-axis terminal and field winding voltages
i_d, i_q, i_f	pu	d-axis, q-axis armature and field winding currents
i_D, i_{Q1}, i_{Q2}	pu	d- and q-axes damper winding currents
l_D,l_f	pu	d-axis damper and field winding fluxes
l_{Q1}, l_{Q2}	pu	q-axis damper winding fluxes
r_D,r_f	pu	d-axis damper and field winding resistances
r_{Q1},r_{Q2}	pu	q-axis damper winding resistances
l_{AD}, l_{AQ}	pu	d- and q-axes mutual fluxes
M_d, M_q	pu	d- and q-axes mutual inductances
T_E	N m	electrical torque
T_M	N m	mechanical torque
Θ	rad	generator rotor angle
ω	rad/sec	generator rotor angle speed
ω_o	rad/sec	rated generator rotor angle speed

Table 5.1: Generator Model Variable Definitions

5.2 Speed Governor Model

To provide the mechanical torque and mechanical power variables during the dynamic simulations, the turbine/speed governor model shown in Figure 5.1 was used [34]. The model

comprises a single simple-lag block, two lead-lag blocks and an input torque limiter. Based on this diagram, the equations that describe the turbine/speed-governor for each machine are given by

$$Tm = Pm/\omega \tag{5.11}$$

$$\dot{P}m = \frac{T_4}{T_5}\dot{A}_4 + \left(A_4 - Pm\right)\frac{1}{T_5} \tag{5.12}$$

$$\dot{A}_4 = \frac{T_3}{T_C}\dot{A}_2 + \left(A_2 - A_4\right)\frac{1}{T_C} \tag{5.13}$$

$$\dot{A}_2 = \left(TMin - A_2\right)\frac{1}{T_S} \tag{5.14}$$

$$TMin = \begin{cases} TMAX & if \quad TMI \geq TMAX \\ TMIN & if \quad TMAX > TMI > 0 \\ 0 & if \quad TMI \leq 0 \end{cases} \tag{5.15}$$

$$TMI = K(1-\omega) + Tm \tag{5.16}$$

The parameters for each machine are T_S = 0.1, T_3 = 0.0, T_C = 0.5, T_4 = 1.25, T_5 = 5.0, TMAX = 1.0 and K = 25.

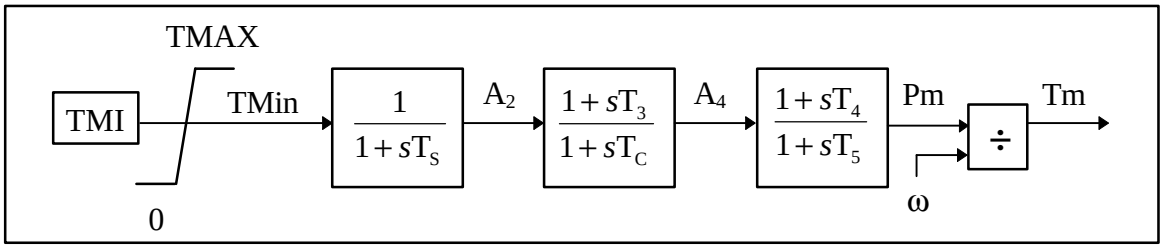

Figure 5.1: Turbine and Speed Governor Model

5.3 Excitation System Models

Two different types of exciters (AVRs) were used for the test system generators. For the machines without PSSs, a simple-gain exciter was employed. For this model, the control equation is written as

$$EFD_{out} = \begin{cases} EFD_{max} & if \quad E_{FD} \geq EFD_{max} \\ E_{FD} & if \quad EFD_{max} > E_{FD} > EFD_{min} \\ EFD_{min} & if \quad E_{FD} \leq EFD_{min} \end{cases} \tag{5.17}$$

where

$$E_{FD} = K\left(V_{ref} - V_C\right) \quad or \quad \dot{E}_{FD} = -K\dot{V}_C \tag{5.18}$$

The parameters for the simple-gain model are K = 200, EFD_{max} = 20 and EFD_{min} = -10.0. For the machines with a PSS, the IEEE ST1-Type exciter shown in Figure 5.2 was used [30]. The control equations are given by

$$V_E = V_{ref} + VPSS - V_C - V_F \tag{5.19}$$

$$V_F = \left(KF/TF\right)V_R - V_{FL} \tag{5.20}$$

$$\dot{V}_{FL} = \left(KF/TF\right)V_R - V_{FL} \tag{5.21}$$

$$\dot{V}_{FL} = V_F \tag{5.22}$$

$$V_I = \begin{cases} VI_{max} & if \quad V_E \geq VI_{max} \\ V_E & if \quad VI_{max} > V_E > VI_{min} \\ VI_{min} & if \quad V_E < VI_{min} \end{cases} \tag{5.23}$$

$$\dot{V}_R = \frac{KAV_I - V_R}{TA} \tag{5.24}$$

$$\dot{E}_{FD} = \begin{cases} EFD_{max} & if \quad \dot{V}_R \geq EFD_{max} \\ \dot{V}_R & if \quad EFD_{max} > \dot{V}_R > EFD_{min} \\ EFD_{min} & if \quad \dot{V}_R < EFD_{min} \end{cases} \tag{5.25}$$

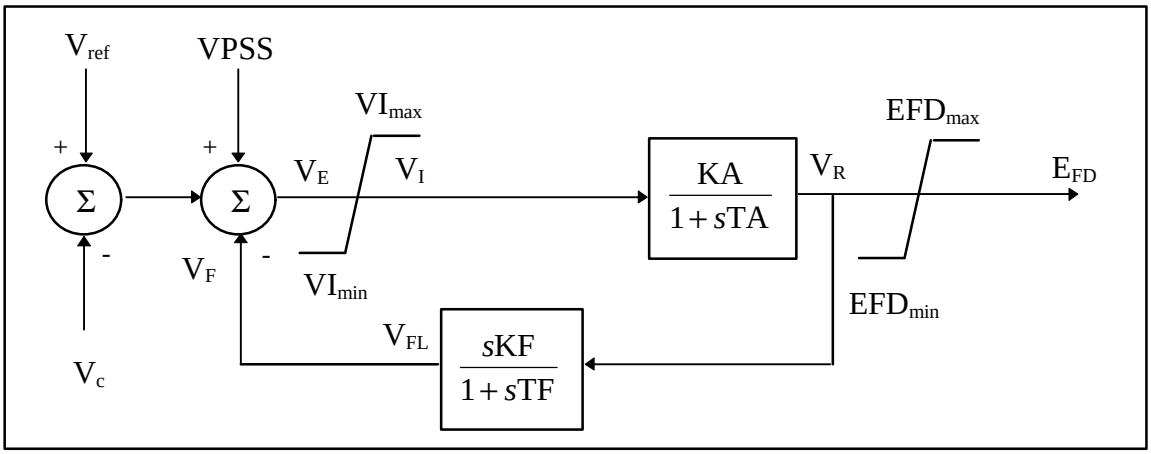

Figure 5.2: ST1-Type Exciter with PSS Input [33]

For both types of AVRs, the terminal voltage (V_C), as depicted in Figure 5.3, is a function of the *d*- and *q*-axis voltages, which, in turn, depend on the real and imaginary portions of the voltage at the terminals (V_R, V_I), the current through the machine connection node (IR, II) and the

impedance seen from the machine ($R_C + jX_C$). The complete equation set for the terminal voltage control block is given by

$$\dot{V}_C = \left(VCB - V_C\right)\frac{1}{T_R} \tag{5.26}$$

$$VCB = \sqrt{\left(V_R + I_R X_C + I_I R_C\right)^2 + \left(V_I + I_R X_C + I_I R_C\right)^2} \tag{5.27}$$

$$\begin{bmatrix} I_R \\ I_I \end{bmatrix} = \begin{bmatrix} \sin\theta & \cos\theta \\ -\cos\theta & \sin\theta \end{bmatrix} \times \begin{bmatrix} i_d \\ i_q \end{bmatrix} \tag{5.28}$$

where i_d and i_q are the *d*-axis and *q*-axis currents, respectively.

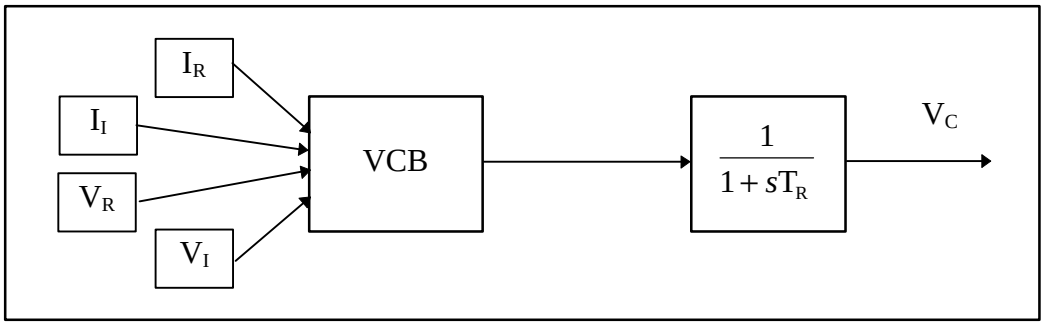

Figure 5.3: Terminal Voltage Control Block

5.4 Power System Stabilizer

The lead-lag PSS structure shown in Figure 5.4 was used. The control equations for this PSS are given by

$$\dot{V}_{PSS} = \begin{cases} VPSS_{max} & if \quad \dot{V}_5 \geq VPSS_{max} \\ \dot{V}_5 & if \quad VPSS_{max} > \dot{V}_5 > VPSS_{min} \\ VPSS_{min} & if \quad \dot{V}_5 \leq VPSS_{min} \end{cases} \tag{5.29}$$

$$\dot{V}_5 = K_S \dot{V}_3 - \frac{V_5}{T_W} \tag{5.30}$$

$$\dot{V}_3 = \frac{T_3}{T_4}\dot{V}_1 + \frac{V_1 - V_3}{T_4} \tag{5.31}$$

$$\dot{V}_1 = \frac{T_1}{T_2}\Delta\dot{I}nput + \frac{\Delta Input - V_1}{T_2} \tag{5.32}$$

$$\Delta\text{Input} = \begin{cases} \Delta\omega = \omega_{mach} - \omega_o \\ or \\ \Delta Pa = P_{mech} - P_{elec} \end{cases} \tag{5.33}$$

The parameters for the PSSs used in this thesis are given in Table 6.9, located in Section 6.3.2.

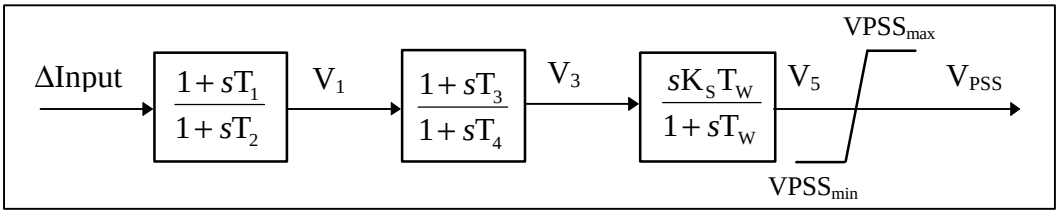

Figure 5.4: Lead-Lag Power System Stabilizer [23]

5.5 Linearized State Equations

Now that all of the nonlinear state equations describing the system have been written, the linearization of the state equations must be performed to yield the final form of the state space system that is used in the small-signal stability analysis and the dynamic simulations. Concurrent with the linearization, elimination of the non-state variables and equations from the generator model is performed. The nonlinear equations for the generators, namely (5.3-5.6) and (5.9-5.10), are kept as the state space model, with the elimination of the *d*- and *q*-axis current variables completed by using (5.1), (5.2), (5.7) and (5.8). Passage from the (d, q) generator reference frame to the (R, I) network reference frame is accomplished through the transformed current (5.28) and the transformed voltage. The latter is written as

$$\begin{bmatrix} V_R \\ V_I \end{bmatrix} = \begin{bmatrix} \sin\Theta & \cos\Theta \\ -\cos\Theta & \sin\Theta \end{bmatrix} \begin{bmatrix} v_d \\ v_q \end{bmatrix} \tag{5.34}$$

where V_R and V_I are the real and imaginary components of the network reference frame and Θ is the angle between the network and rotor reference frames.

The complete set of state equations in matrix-vector form for the system including a machine is now given by

$$\begin{bmatrix} \Delta\dot{\lambda}_f \\ \Delta\dot{\lambda}_D \\ \Delta\dot{\lambda}_{Q1} \\ \Delta\dot{\lambda}_{Q2} \\ \Delta\dot{\omega} \\ \Delta\dot{\Theta} \end{bmatrix} = \begin{bmatrix} 0 & a_{12} & a_{13} & a_{14} & a_{15} & a_{16} \\ 0 & a_{22} & a_{23} & a_{24} & a_{25} & a_{26} \\ 0 & a_{32} & a_{33} & a_{34} & a_{35} & a_{36} \\ 0 & a_{42} & a_{43} & a_{44} & a_{45} & a_{46} \\ 0 & a_{52} & a_{53} & a_{54} & a_{55} & a_{56} \\ a_{61} & 0 & 0 & 0 & 0 & 0 \end{bmatrix} \begin{bmatrix} \Delta\lambda_f \\ \Delta\lambda_D \\ \Delta\lambda_{Q1} \\ \Delta\lambda_{Q2} \\ \Delta\omega \\ \Delta\Theta \end{bmatrix} + \begin{bmatrix} 0 & b_{12} \\ 0 & 0 \\ 0 & 0 \\ 0 & 0 \\ b_{41} & 0 \\ 0 & 0 \end{bmatrix} \begin{bmatrix} \Delta Tm \\ \Delta EFD \end{bmatrix} \quad (5.35)$$

The equations for the simple-gain exciter from (5.18), the speed-governor control blocks from (5.11-5.16) and the terminal voltage control block from (5.26-5.28) are not shown in this model. The **A**- and **B**-matrix matrix coefficient expansions for the system shown in (5.35) can be found in Appendix A, while the complete **A**-matrix coefficients are shown for the base case load flow in Appendix B.

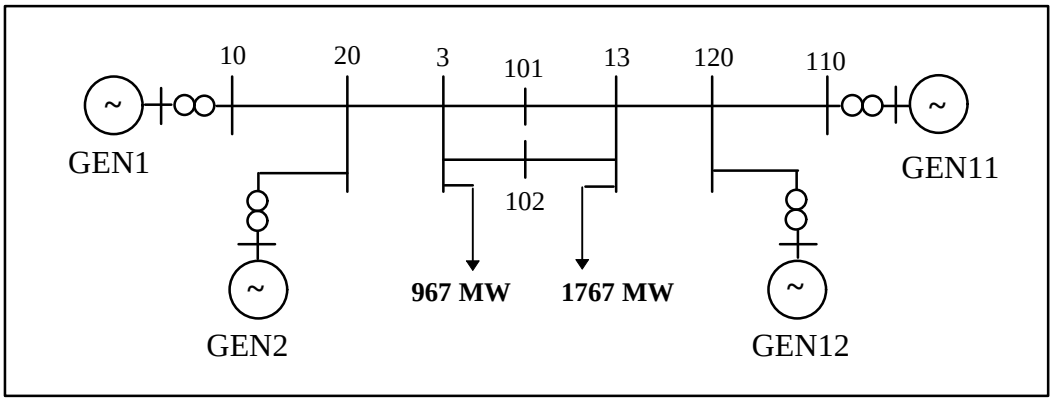

Figure 5.5: Two Area, 4-Machine Test System

5.6 Test System

The one-line diagram of the two-area, 4-machine test system used to examine the inter-area oscillation control problem is shown in Figure 5.5. Originally a 6-bus system in [1], the system has been modified by the addition of transformers between each generator and the transmission lines, and now closely resembles the 4-machine system from [11]. In fact, this system was created especially for the analysis and study of the inter-area oscillation problem [1,11]. This system has become a reference test system for studying the inter-area oscillation control problem, much like the 3-machine system from [33] or the "New England" 10-machine system [35] have served as references for other studies requiring a common, accessible test system.

Visible in the one-line diagram are the four generators, GEN1, GEN2, GEN11 and GEN12, and their associated 20kV/230kV step-up transformers. There are two loads in the system at buses 3

and 13. The transformer and line impedances for the system are given in Table 5.2, while the generation, load and voltage data is enumerated in Table 5.3. The per-unit values were calculated on a 100MVA base.

From Bus	To Bus	R (pu)	X (pu)	B/2 (pu)
GEN1	10	0.0	0.0167	--
GEN2	20	0.0	0.0167	--
GEN11	110	0.0	0.0167	--
GEN12	120	0.0	0.0167	--
10	20	0.0025	0.025	0.021875
20	3	0.001	0.01	0.00875
3	101	0.011	0.11	0.09625
3	102	0.011	0.11	0.09625
101	13	0.011	0.11	0.09625
102	13	0.011	0.11	0.09625
13	120	0.001	0.01	0.00875
120	110	0.0025	0.025	0.021875

Table 5.2: Impedance Data for 4-Machine System

Generator or Load	Voltage Magnitude (per unit)	Voltage Angle (degrees)	Real Power (MW)	Reactive Power (MVAR)
GEN1	1.03	18.56	700	185
GEN2	1.01	8.8	700	235
GEN11	1.03	-8.5	719	176
GEN12	1.01	-18.69	700	202
Load 3	0.96	-6.4	967	100
Load 13	0.97	-33.86	1767	100

Table 5.3: Initial Generation and Load Data for 4-Machine System

Many assumptions are needed to place the power system models into service for the small-signal analysis. The loads were modeled as constant impedances. The generators were described using the two-axis model discussed in [11] and [30] given in Section 5.1, and the turbine and speed governor model from Section 5.2. The excitation system for each of the generators was also modeled in detail, along with any additional controllers, as shown in Sections 5.3 and 5.4. Finally, to complete the state matrix formulation, all of the state variables and equations were linearized around an initial operating point, as developed in Section 5.5.

The external parameters of the generators are given in Table 5.4, while Table 5.5 contains the exciter parameters. The initial conditions are calculated internally by EUROSTAG. However, it is also possible to calculate these values given the generator external parameters and the load flow results using MATLAB [36] with the program "initcond.m" (Appendix C.1), containing the equations for the method used by EUROSTAG to calculate the initial conditions. The internal machine parameters, consisting of the resistances and inductances, are first calculated from the set

of external parameters, including the reactances and time constants. The load flow information, consisting of the real and reactive power generated, the machine connection bus voltage and the angle of the voltage, is then used to calculate the initial conditions of the state variables. Based on this approach, Table 5.6 contains the internal parameters of the generators and Table 5.7 the initial conditions.

Parameter	Generators 1, 2	Generators 11, 12
x_d	1.8	1.8
x'_d	0.3	0.3
x''_d	0.25	0.25
x_q	1.7	1.7
x'_q	0.55	0.55
x''_q	0.25	0.25
Ra	0.0025	0.0025
Xl	0.2	0.2
T'_{do}	8.0	8.0
T''_{do}	0.03	0.03
T'_{qo}	0.4	0.4
T''_{qo}	0.05	0.05
H	6.5	6.175

Table 5.4: External Parameter Generator Data

Parameter	Value
KA	345.1265
TA	0.0116
KF	0.0551
TF	2.1511
VI_{max}	12.137
VI_{min}	-12.137
EFD_{max}	Vterm(12.137) - Ifield
EFD_{min}	Vterm(-12.137) + Ifield
RC	0.0
XC	0.0
TR	0.01

Table 5.5: ST1-Type Exciter Data

Parameter	Gen 1,2, 11,12,
Ra	0.0025
Ld	0.2
Lq	0.2
r_f	0.0006
r_D	0.0172
r_{Q1}	0.0231
r_{Q2}	0.0241
L_f	0.1123
L_D	0.0955
L_{Q1}	0.0547
L_{Q2}	0.9637
M_d	1.6
M_q	1.5

Table 5.6: Internal Machine Parameters

Parameter	Gen 1	Gen 2	Gen 12	Gen 11
UR_o	-0.2941	0.5908	0.1065	-0.8224
UI_o	0.9871	-0.8192	0.9972	-0.6201
IR_o	-0.0267	0.2648	0.3749	-0.8052
II_o	0.8569	-0.8511	0.7957	-0.3461
ud_o	-0.9953	0.9572	-0.97	1.0
uq_o	0.6927	-0.2182	1.0464	-0.5672
id_o	-0.1045	0.1087	0.1073	0.1069
iq_o	0.1044	-0.0896	0.0682	0.0737
Θ_o	0.0293	0.3	-0.442	-1.1667
λad_o	0.0191	-0.0212	0.0187	-0.0199
λaq_o	0.0235	-0.0205	0.0162	0.0121
$\lambda Q1_o$	0.0235	-0.0205	0.0162	0.0121
$\lambda Q2_o$	0.0235	-0.0205	0.0162	0.0121
λd_o	0.1355	-0.1431	0.1376	-0.1392
λq_o	0.0322	-0.0349	0.032	-0.0333
if_o	0.1165	-0.1219	0.1189	-0.1193
efd_o	-0.1863	0.1951	-0.1903	0.1909
tm_o	-0.0005	-0.0005	-0.0004	0.0003

Table 5.7: Generator Initial Conditions

EUROSTAG was also used to perform the small-signal and time-domain analyses. In brief, this package calculates the load flow based on the topological data of the power system, then uses the parameters of the machines in the system coupled with the load flow results to perform the time-domain simulations. While small-signal analysis is not included in the operational functions of this package, it is possible to save the state-space model at any instant in time during the dynamic simulations in a format compatible with that of MATLAB [32]. The use of MATLAB in conjunction with EUROSTAG provides the tools needed to complete the analysis of the research performed in this thesis.

There are, however, several drawbacks to using the two software packages in this manner. It is not possible to explicitly see the state equations as they are used in the eigenvalue calculation and the time-domain simulation. However, it is possible to write all of the equations describing the machines and their interactions used by the software. While the **Y**-bus matrix is also not available as a EUROSTAG output, the derivation of this matrix can be performed in the manner described in [33]. The discussion of a multi-machine stability problem is given in [33] as well, and this reference is quoted by the EUROSTAG programmers [30, 32].